$S=\frac{1}{2}$ Ising behavior in the two-dimensional molecular magnet $Fe(NCS)_2(pyrazine)_2$

H. N. Bordallo,[1,2,*] L. Chapon,[1,3,†] J. L. Manson,[4,5] J. Hernández-Velasco,[1] D. Ravot,[6] W. M. Reiff,[7] and D. N. Argyriou[1]

[1]*Hahn-Meitner Institut, Glienicker Straβe 100, 14109 Berlin, Germany*

[2]*Intense Pulsed Neutron Source, Argonne National Laboratory, Argonne, Illinois 60439, USA*

[3]*ISIS Department, Rutherford Appleton Laboratory Chilton, Didcot OX11 0QX, United Kingdom*

[4]*Center for Neutron Scattering, Oak Ridge National Laboratory, Oak Ridge, Tennessee 37831, USA*

[5]*Department of Chemistry and Biochemistry, Eastern Washington University, 226 Science Building, Cheney, Washington 99004, USA*

[6]*Laboratoire de Physicochimie de la Matière Condensée, UMR 5617 CNRS, Université Montpellier II, 5 place E. Bataillon, 34095 Montpellier Cedex 5, France*

[7]*Department of Chemistry, Northeastern University, Boston, Massachusetts 02115, USA*

(Received 27 January 2004; published 10 June 2004)

The magnetic ordering and critical behavior of antiferromagnetic $Fe(NCS)_2(pyrazine)_2$ has been studied by neutron powder diffraction (NPD), inelastic neutron scattering (INS), Mössbauer spectroscopy, and magnetic measurements. The system can be regarded as a two-dimensional (2D) antiferromagnet even in the ordered phase, given that long-range magnetic ordering between the layers simply follows a necessary consequence of the establishment of long-range ordering within the planes. The INS data, which were taken on a cold neutron time-of-flight spectrometer, reveals that when the temperature is lowered towards T_N, the correlation length within the 2D layers increases and ultimately crosses over from two- to three-dimensional (3D) behavior. Indeed, 3D long-range antiferromagnetic order, associated with a propagation vector $[1,0,\frac{1}{4}+\epsilon]$, is observed in the NPD data below 6.8 K. Furthermore, in agreement with the behavior of both $\chi(T)$ and $C_m(T)$ data, the order parameter follows the exact Osanger solution for a 2D $S=1/2$, Ising system.

DOI: 10.1103/PhysRevB.69.224405 PACS number(s): 75.50.Xx, 61.12.−q, 75.50.Ee, 75.25.+z

I. INTRODUCTION

In the past decade, spectacular advances have been made in the field of molecular magnetism with the promise of readily designed magnetic systems.[1] An essential approach to provide molecule-based materials exhibiting spontaneous magnetization is to construct ordered extended structures with superexchange interactions between the metal centers.[2] For example, potential bridging ligands such as pyrazine ($C_4N_2H_4$,pyz), provide efficient superexchange pathways. This ligand coordinates to metal ions in a bis-monodentate fashion through its two nitrogen lone pairs leading to intramolecular metal-metal separations of about 6.8–7.5 Å, assembling one-dimensional (1D) linear chains or two-dimensional (2D) layer compounds.[3–7] The most extensively studied complexes of this type have been copper(II), where it has been found that an important factor in determining the nature of the exchange interactions is an effective d(metal)-π(pyz) overlap. Overall, the interaction through this ligand is weak, and discrepancies between theoretical predictions and experimental results can be attributed to the fact that the calculations overemphasize the intermolecular overlap.[8,9] Nevertheless, many systems using pyz (or its derivatives) as a building block display antiferromagnetic ordering ranging from a few Kelvin up to 62 K.[10–12]

In this work we have focused on $Fe(NCS)_2(pyz)_2$ that has been characterized as a 2D sheetlike polymer by Real *et al.*,[6] where the thermal variation of its magnetic susceptibility, a broad maximum at 8.5 K, suggests an antiferromagnetic ground state at low temperature. Furthermore, Mössbauer spectroscopy studies show that below 8.4 K the spectra are hyperfine split, although with very broad lines. This observation results from relaxation effects that are occurring within the Mössbauer frequency window (10^{-7} s^{-1}), which may arise either from slow single-ion relaxation effects or from soliton (domain wall) motion. The line broadening persists down to about 7 K, and between 7 and 9 K, satisfactory simulations of the spectra could not be achieved by using a static molecular field, preventing an accurate determination of the Néel temperature.[13]

Using neutron powder diffraction (NPD) we were able to demonstrate that $Fe(NCS)_2(pyz)_2$ shows three-dimensional (3D) long-range magnetic ordering below 6.8 K. The magnetic structure consists of Fe spins antiferromagnetically ordered in the *ab* plane, exhibiting a sinusoidal modulation along the *c* axis with the quasicommensurate propagation vector $[1,0,\frac{1}{4}+\epsilon]$. Furthermore, detailed diffraction measurements show that below T_N the sublattice magnetization varies as $|T\text{-}T_N|^{\beta}$ with $\beta \simeq 0.19$.

In order to understand the apparent 2D behavior of the magnetic ordering of $Fe(pyz)_2(NCS)_2$, we combined inelastic neutron scattering (INS) with magnetic specific heat measurements (C_m). Between 7 and 50 K, magnetic fluctuations, with a gap of about 1 meV, are observed in the INS spectra. This finding indicates very-long-range correlations within the planes, with no measurable correlations between the planes. In addition, in the vicinity of the critical temperature, C_m can be well described using the Onsager prediction for a 2D Ising square system.[14] Accordingly, we conclude that even in the ordered phase the magnetic behavior is predominantly 2D in character.

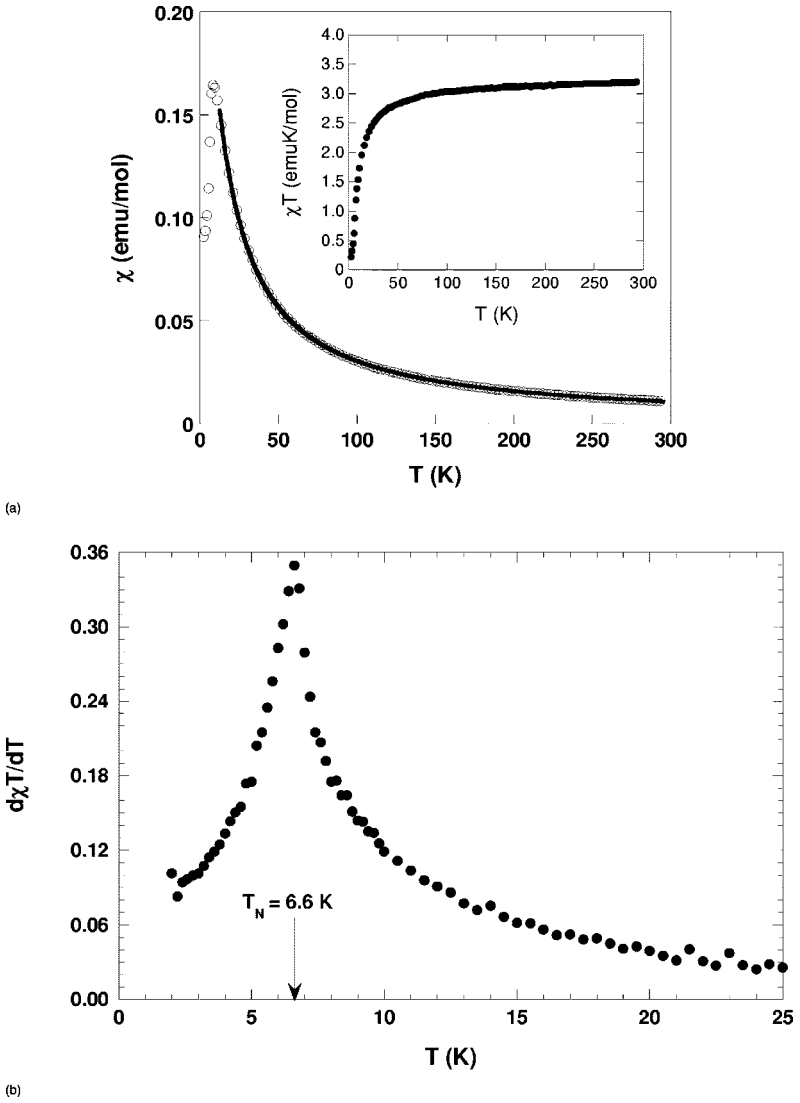

FIG. 1. (a) Plot of $\chi(T)$ suggesting that short-range ordering within the 2D layers takes place below 9 K. The inset of the figure $\chi T(T)$ gives further evidence of antiferromagnetic correlations between the Fe^{2+}. (b) Plot of the derivative of $\chi T(T)$ with respect to the temperature. The observation of a sharp peak indicates the onset of a 3D magnetic ordered phase.

II. EXPERIMENTAL

A per-deuterated polycrystalline sample of $Fe(NCS)_2(pyz)_2$ was prepared by the following procedure: A 10-mL aqueous solution of $FeSO_4 \cdot 7H_2O$ (Aldrich; 4.086 g, 14.7 mmol) was added while stirring to a 10-mL aqueous solution containing NH_4NCS (Baker; 2.350 g, 30.9 mmol) and pyz-d_4 (Aldrich; 2600 g, 30.8 mmol). An orange-brown solid precipitated immediately. The mixture was stirred for an additional 1 h to ensure a complete reaction. The solid was collected via suction filtration and dried *in vacuo* for 12 h to yield 4.750 g of $Fe(NCS)_2(pyz\text{-}d_4)_2$ in 95% yield. Sample identity and purity were established by infrared and Mössbauer spectroscopies. The measured x-ray powder diffraction pattern matched that calculated from the known crystal structure.[6]

Neutron powder diffraction (NPD) was used to probe the crystal and magnetic structures of $Fe(NCS)_2(pyz\text{-}d_4)_2$ as well as to follow the ordering of Fe spins close to T_N. NPD patterns were measured in the temperature range 4–300 K using the special environment powder diffractometer (SEPD) time-of-flight powder diffractometer at the Intense Pulsed Neutron Source (IPNS), Argonne National Laboratory. For the solution of the magnetic structure, additional measurements were performed between 2 and 10 K using the *E*9 neutron powder diffractometer at the Hahn-Meitner Institut (HMI) and the OSIRIS spectrometer at the ISIS facility, Rutherford Laboratory. In order to follow the evolution of the magnetic superlattice reflections as a function of temperature, relevant portions of the diffraction pattern were measured from 1.4 to 10 K at 0.2 K intervals using the *E*6 neutron powder diffractometer at HMI. The NPD data were analyzed by the Rietveld method using the GSAS[15] suite of programs and FULLPROF.[16]

INS experiments were performed on 3.54 g of a deuterated powder sample with the high-resolution multichopper time-of-flight spectrometer NEAT at HMI. Data were collected at different temperatures, between 2 and 50 K, with an incident neutron energy of 3.15 meV ($\lambda = 5.1$ Å), giving a resolution of 217 μeV at the elastic peak position. [17] The usual data treatment procedure has been followed to correct the data for absorption and detector efficiency and normalization runs have been determined by comparing to an empty-can run.

The heat capacity has been measured by the relaxation method using a probe and a cryostat manufactured by Oxford Instruments. A 1 mg polycrystalline sample compacted into a dense pellet was affixed on a small platform suspended in a vacuum with a weak thermal link to the heat bath. The heat capacity is expressed as the ratio between time relaxation and the thermal resistance.

Mössbauer spectra were determined using a conventional constant acceleration spectrometer operated in multichannel scaling mode. The gamma ray source consisted of a 25 mCi of ^{57}Co in a rhodium metal matrix that was maintained at ambient temperature. The spectrometer was calibrated using a 6-μm-thick natural abundance iron foil. The velocity scale is relative to the center of the magnetic hyperfine pattern of the latter foil taken as zero velocity. The line widths of the innermost pair of $\Delta M_I = \pm 1$ transitions of the latter Zeeman pattern were reproducibly determined to be 0.214 mm/s. Sample temperature variation was achieved using a standard exchange gas liquid helium cryostat (Cryo Industries of America, Inc.) with temperature measurement and control based on silicon diode thermometry in conjunction with a 10-μA excitation source (Lakeshore Cryotronics, Inc). Samples ($\approx$25 mg of polycrystalline powder) were bulked with apiezon -*N* grease to insure good thermal contact in sealed nylon holders.

III. RESULTS

A. Magnetic susceptibility

Characterization of both deuterated and nondeuterated samples using magnetic susceptibility measurements show essentially identical behavior and confirm some of the initial measurements made on this material.[6,13]

We find that while the broadness of $\chi(T)$ [Fig. 1(a)] suggests that short-range ordering within the 2D layers takes place below 9 K, the existence of antiferromagnetic correlations between Fe^{2+} centers is indicated by the decreasing nature of $\chi(T)(T)$ [see the inset of Fig. 1(a)]. The value of $\chi(T)(T)$ at 300 K suggests that the Fe^{2+} site is in a high-spin $S=2$ ground state, although the observed value of 3.19 emu K/mol is larger than expected for g=2.0, i.e., 3 emu K/mol. A fit of the reciprocal magnetic susceptibility data to a Curie-Weiss expression gives an anisotropic *g* value of 2.09(1) and $\theta=-8.36(4)$ K. A deviation from the linear Curie-Weiss fit is observed below 25 K reflecting the development of short-range correlations. Similar behavior was previously observed in other Ising systems.[18]

The occurrence of a sharp peak in the plot of the derivative of $\chi(T)(T)$ vs T would indicate the onset of a 3D magnetic ordered phase. Indeed, this is what we observe in Fig. 1(b), which shows a peak at 6.6 K that is well below the T_{max} from $\chi(T)$. As will be shown in the following subsections, the T_N obtained from bulk magnetic measurements agrees quite well with those obtained from the heat capacity, neutron scattering, and Mössbauer studies. From our knowledge of T_N and θ, we obtain $T_N/\theta=0.789$.

B. Crystal Structure

The resulting crystal structure from the final refinement of the NPD data is shown in Fig. 2. At 300 K, the material

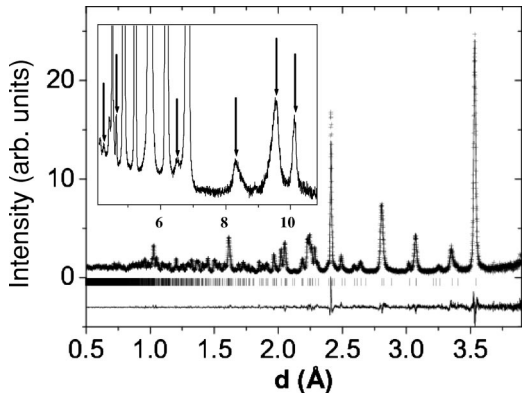

FIG. 2. Rietveld refinement of the back-scattering bank data collected on SEPD for $Fe(NCS)_2(pyz\text{-}d_4)_2$ at room temperature. The cross and the solid line represent, respectively, the experimental data and the result of the refinement. The vertical bars mark the positions of the Bragg reflections. The solid line at the bottom is the residual between the experimental and calculated patterns. The insert shows the magnetic structure at 2 K. The arrows indicate the magnetic reflections.

crystallizes in the monoclinic space group $C2/m$ with $a=10.1975(2)$ Å, $b=10.4479(2)$ Å, $c=7.1745(3)$ Å and $\beta=118.785(2)°$. The refinement leads to an excellent agreement factor ($R_{wp}=0.0487$, $\chi^2=1.63$ and $R_{(F^2)}=0.0510$) and is consistent with the previous structure established from single crystal x-ray diffraction.[6] Tables I and II display, respectively, atomic positions at room temperature and cell parameters at selected temperatures.

The structure (Fig. 3) may be described as a parallel stacking of sheets along the *c* axis organized in the *ab* plane. Each sheet consists of a slightly distorted square array of Fe^{2+} ions, two neighboring Fe ions being connected by a pyrazine molecule via its nitrogen atoms leading to a intrasheet Fe-Fe distance of 7.299 Å. The distortion is such that the four Fe-Fe distances remain equivalent while the angles of the initial square slightly reduce the symmetry of the motif to a diamond with an angle of 91.390(2)°. The pyrazine ligands are canted toward the *c* direction and thus do not lie in the *ab* plane. The two NCS^- counteranions are terminally bonded to the Fe center and stand above and below the sheet in an almost perpendicular fashion. As a result, the Fe ion is a six coordinate with four long equatorial Fe-N_1 bonds [2.268(2) Å] and two short axial bonds Fe-N_2(2.053 Å). The angles within the axially compressed octahedra deviate slightly from 90°. Consequently, the local symmetry around the Fe atom is formally D_{2d}. However, to a first approximation it remains very close to D_{4h}. The sheets alternate and the Fe atom of a given sheet lies vertically above the center of the diamond formed by four Fe atoms in adjacent sheets. The intersheet Fe-Fe separation is 7.174 Å and slightly smaller than the intrasheet one. Neither covalent bonds nor dative bonds connect adjacent sheets, and the shortest distance between them is the terminal sulfur of the thiocyanate pointing towards an iron atom of the next sheet at 4.679 Å. This lack of a strong chemical connection between the layers motivated the description of this compound as a "2D sheetlike polymer,"[6] and our interest in this system.

TABLE I. Atomic coordinates and atomic displacement parameters (ADP) for $Fe(NCS)_2(pyz\text{-}d_4)_2$ at room temperature. The annotation *c* refers to constrained parameters in the refinement.

Atom type	*x*	*y*	*z*	$U^2_{eq}\times 10^2(\text{Å}^2)$
Fe	0	0	0	1.2(3)
N(1)	0.1577(3)	0.1553(2)	0.0063(5)	2.5(2)
N(2)	0.1109(5)	0	0.3264(8)	2.8(3)
C(1)	0.2095(7)	0	0.4976(11)	2.6(4)
C(2)	0.2062(5)	0.3250(4)	−0.1714(8)	$3.68(9)^{c1}$
C(3)	0.1153(5)	0.2297(5)	−0.1596(8)	$3.68(9)^{c1}$
S	0.3462(7)	0	0.748(4)	9.67(15)
D(1)	0.3344(7)	0.1087(6)	0.3021(10)	$7.94(13)^{c2}$
D(2)	0.0024(7)	0.2194(6)	0.2984(9)	$7.94(13)^{c2}$

Further evidence that the sheets are loosely connected is given by anisotropic peak broadening in the NPD data. Accordingly, the only reasonable refinement was achieved by using a peak profile function that included anisotropic Lorenztian broadening (an order 2 tensor $L_{ij}1\leqslant i,j\leqslant 3$). While the parameters L_{11} and L_{22} are nearly resolution limited, L_{33} is significantly larger ($L_{33}\simeq 3\times L_{11}=3L_{22}$), consistent with the observation of stacking faults along the c axis.[19] On cooling, no symmetry lowering is observed. The structure can be described with the same monoclinic space group and the anisotropic broadening does not vary. However, a weak contraction of the *b* axis is observed below 8 K, while no anomalies were detected in the *T* dependence of the *a* and *c* axis. This behavior corresponds to a weak contraction of the diamond angle, and because it occurs at a temperature close to the maximum observed in the magnetic susceptibility, it may be correlated to the onset of spin ordering in the 2D lattice.

C. Critical behavior

A principal point of interest is of course the question of whether in the magnetically ordered phase, $Fe(NCS)_2(pyz\text{-}d_4)_2$ will show the characteristics of a 2D system or if it simply resembles a 3D model.

1. Zero-field magnetic structure

Below 6.8 K, nine additional magnetic reflections are detected in the NPD data (see insert of Fig. 2). These superlattice (SL) reflections are consistent with an antiferromagnetic ground state, in agreement with the decrease of the magnetic susceptibiliy at low temperature, while T_N coincides with the sharp peak observed in the $d_\chi T/dT$ plot. The shape of the SL reflections clearly indicate 3D long-range ordering. Due to the presence of 2D ordering, the magnetic lattice would be described by rods in reciprocal space, and the magnetic scattering in a powder measurement would have a broad sawtoothlike asymmetric profile. Indeed a long tail would be

TABLE II. Unit cell parameters for $Fe(NCS)_2(pyz\text{-}d_4)_2$ at selected temperatures as determined from the SEPD data.

T(K)	*a*(Å)	*b*(Å)	*c*(Å)	$\beta(^\circ)$	$V(\text{Å}^3)$
4	10.1320(2)	10.3967(2)	6.9350(2)	117.387(2)	648.66(2)
25	10.1325(2)	10.3983(2)	6.9381(2)	117.408(2)	648.95(2)
300	10.1975(2)	10.4479(2)	7.1745(3)	118.785(2)	669.94(2)

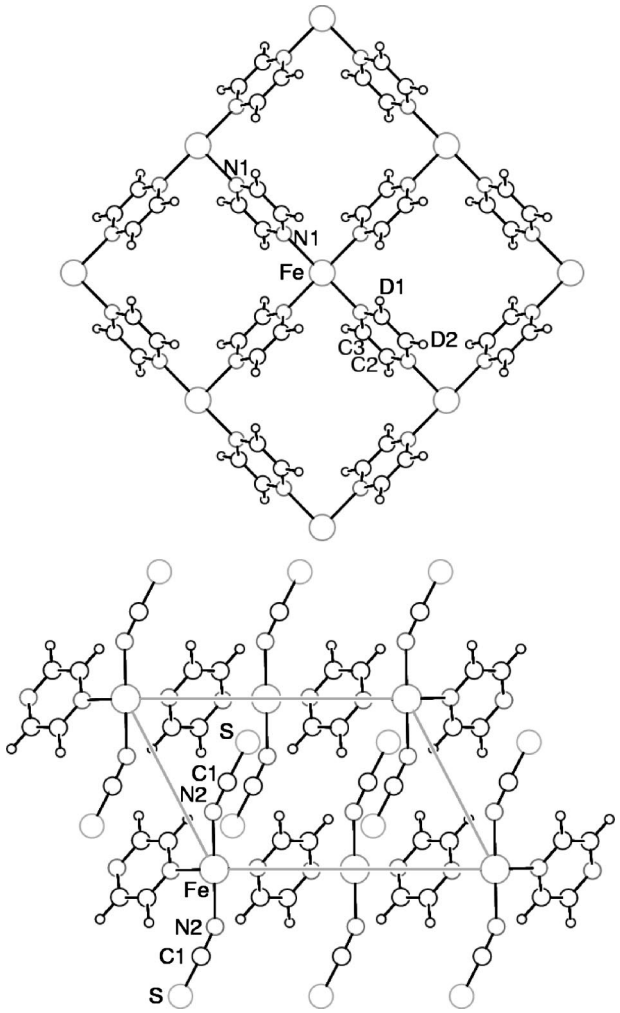

FIG. 3. Nuclear structure of $Fe(NCS)_2(pyz\text{-}d_4)_2$ perpendicular (top) and parallel to (bottom) to the sheets. The gray line marks one unit cell.

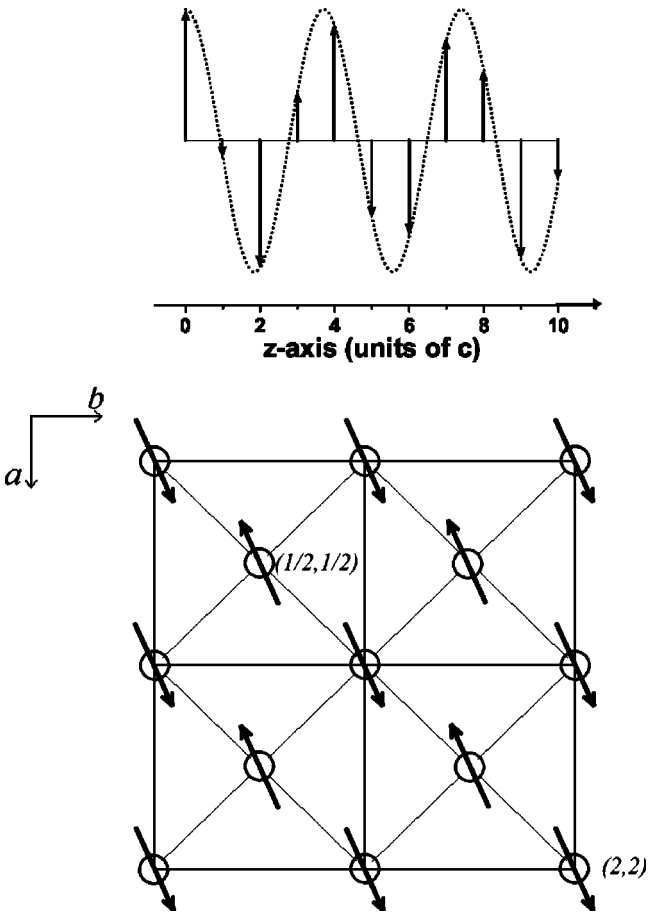

FIG. 4. Spin structure of $Fe(NCS)_2(pyz\text{-}d_4)_2$.

observed on the high-Q side of the peak arising form density of state scattering and well described by a Warren function.[20] Definitely, this is not the case in our measurement as all the magnetic SL peaks have a nearly Gaussian profile. Only one peak at $d=9.47$ Å shows an asymmetric feature, and if likely results from the unresolved convolution of multiple reflections rather than from a pseudocontinuum.

The first attempt to manually index the SL peaks with different propagation vectors failed, thus another approach was used. A starting propagation vector was determined using a modified form of the method of Wilkinson.[21] Here, a

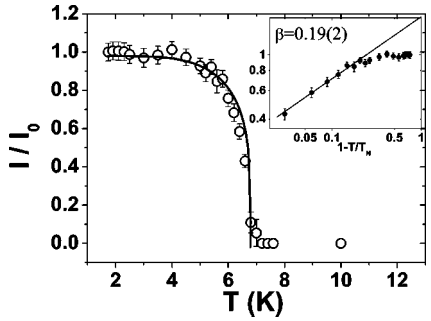

FIG. 5. Integrated intensity of the (200)-τ reflection (square dots). The solid line is a fit of the experimental data to a power law $I/I_0=(1\text{-}T/T_N)^{2\beta}$, with $\beta=0.19$. In the insert, we show the calculation of the critical exponent using the universality hypothesis.[28]

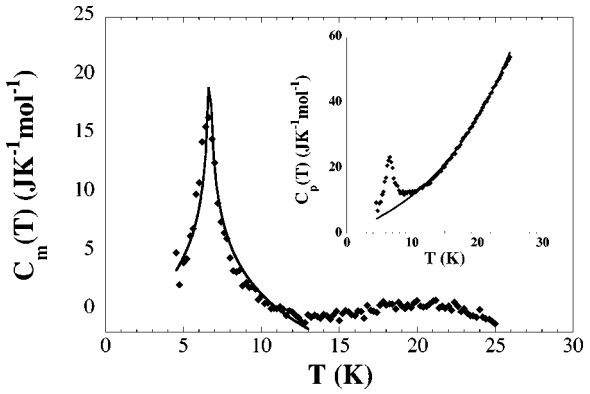

FIG. 6. Magnetic specific heat (C_m) for $Fe(NCS)_2(pyz\text{-}d_4)_2$ at low temperature. The solid line represents the Onsager prediction for a 2D Ising square $S=1/2$ system in the vicinity of the critical temperature, calculated using Eq. (A8). The insert displays the total specific heat measured on the system.

3D grid search was performed, in which the direction of the propagation vector varies throughout a hemisphere of reciprocal space centered at c^* while the magnitude of the vector varies between 0 and $|c^*|/2$. For each propagation vector explored, a figure of merit was calculated based on the weighted root mean square difference between the observed satellite peak positions and the nearest calculated positions. The observed d spacings were obtained through individual fits to each of the well-defined satellite peaks. The observation of three strong peaks in the figure of merit (FOM) map indicates the possible solutions. However, while all these solutions allow an index to the observed SL reflections, only one solution at approximatively $c^*/4$, provides a model that reproduced the satellite peak intensities in our Rietveld refinement. The result of the refinement gave a propagation vector of $\tau=[1,0,0.27(1)]$, which is close to the commensurate value.

Our model of the magnetic structure consists of antiferromagnetic moments aligned in the ab plane and a sinusoidal modulation (transverse wave) of these moments along the c direction as shown in Fig. 4. The sinusoidal modulation of the magnetic structure may be a consequence of some microstructural disorder where a certain degree of frustration arises from the packing sequence.[19] Figure 5 displays the temperature dependence of the integrated intensity of the (200)-τ reflection. The intensity of the magnetic peak depends on the AF staggered magnetization $I(T)\propto|M(T)|^2$. Below T_N, the intensity of this reflection increases abruptly and saturates rapidly to a maximum value. This squarelike dependence of $M(T)$ resembles the behavior expected for 2D systems characterized by a small critical exponent. Indeed, a fit of $M(T)$ in the critical regime gives a critical exponent $\beta=0.19(2)$ that is consistent with the layered nature of the spin system and, in fact, very close to the exact theoretical value of the 2D Ising system,[14] $\beta=0.125$. Similar observations concerning Ni^{2+} and Fe^{2+} have been reported in other layered systems.[22–27]

2. Heat capacity and spin analysis of the sublattice magnetization

In this section, we will first consider the specific heat $[C_m(T)]$ data and then explore the spin-wave results as a

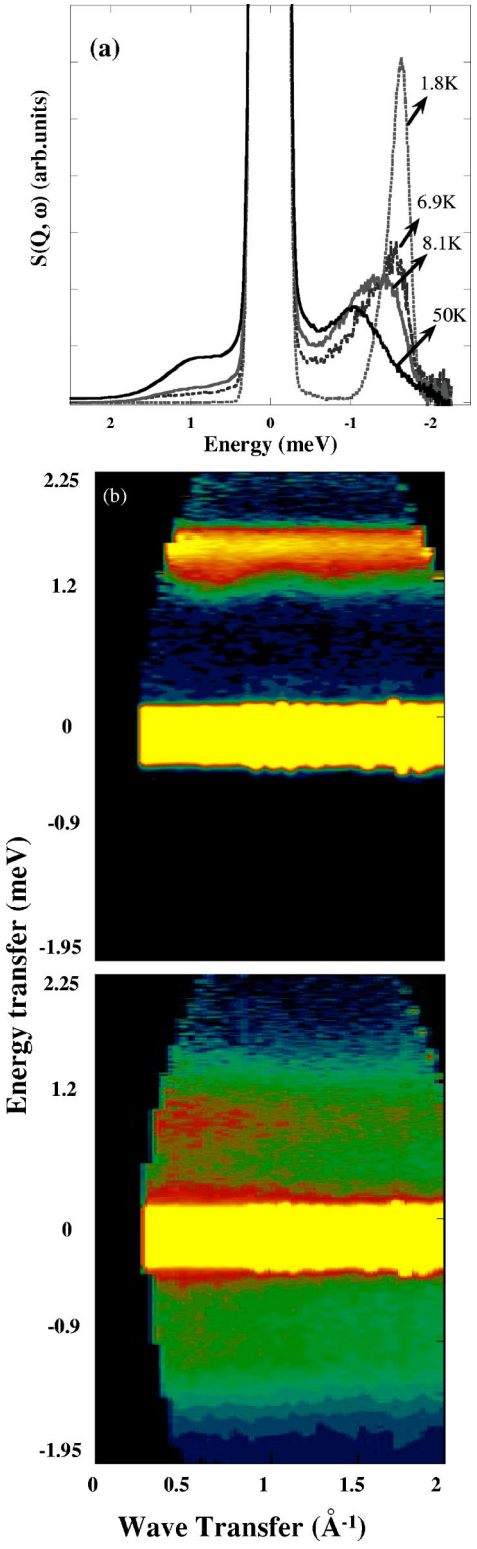

FIG. 7. (a) $S(|Q|,\omega)$ vs energy transfer for $Fe(NCS)_2(pyz\text{-}d_4)_2$ at selected temperatures. Data were taken using $E_0=3.1$ meV($\delta E=217$ μeV) and integrated over the whole Q range (0.4 Å$^{-1}\leqslant Q\leqslant 2.24$ Å^{-1}). Below T_N, besides the elastic peak, a main inelastic response appears at 1.64 meV, which upon heating seems to merge with the peak observed at higher temperatures located at 1.04 meV. (b) (Color online) Energy-momentum spectra at 1.8 and 50 K using NEAT.

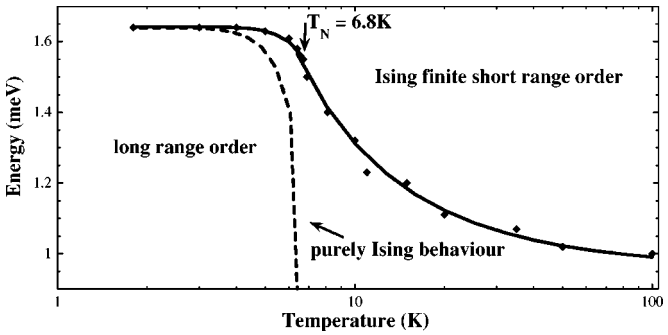

FIG. 8. Evolution of the spin-wave frequency in $Fe(NCS)_2(pyz\text{-}d_4)_2$ vs Temperature. The solid curves are fit to the data using the spin-wave theory as described in the text. The dashed line is the expected temperature dependence of a magnon in a Ising system without crossover from the 2D to the 3D ordering with $T_N=6.8$ K. Above T_N magnetic excitation is observed due to finite correlations in the 2D system.

function of the sublattice magnetization. A summary of the results of the exact solution of the Ising model in 2D that is necessary to the analysis of our experiments is given in the Appendix.[14,29]

The magnetic specific heat (C_m) was calculated by subtracting from the total specific heat, C_p, the electronic and lattice contributions deduced from a fit of the high temperature regime $T\geqslant 12$ K to the law $C_p=\gamma T+aT^3$ (see the inset of Fig. 6). The solid line in Fig. 6 is the best fit to the experimental data obtained using Eq. (A8) for $4.5\leqslant T\leqslant 12$ K, yielding a value for $J=0.25(1)$meV(2.95 K) and $T_N=6.67(2)$K.

To obtain a better global understanding of the 2D magnetic behavior of $Fe(NCS)_2(pyz\text{-}d_4)_2$, INS experiments were performed between 1.8 and 50 K. INS spectra at selected temperatures are shown in Fig. 7. From Fig. 7(a) we observe that the peak ascribed to a spin-wave excitation is sharp well below T_N and rapidly broadens on heating. For $T<T_N$, the observation of a large gap of about 1.64 meV, equivalent to a thermal energy of $3T_N$, as well as no noticeable dispersion of the spin-wave mode [see Fig. 7(b)] is directly associated with the Ising character of the system.[22,30] While in the paramagnetic phase, above T_N, the broadening and the smooth form-factor-like decrease at the large momentum transfer of the magnetic excitation reflects that antiferromagnetic ordering is preserved within the layers on a local scale well above T_N.[26,30]

Moreover, as can be seen in Fig. 8, up to $0.6T_N$, the variation of the spin-wave gap with temperature is comparable to the change of the integrated intensity of the (200)-τ magnetic Bragg reflection. Similar behavior was also observed in the layer compounds K_2NiF_4 and K_2FeF_4.[31–33]

To fit the inelastic data above the Néel temperature, where only short-range ordering is expected, Eqs. (A6) and (A7) were used, giving a J' value of 0.13 meV, which agrees quite well with the value previously reported in the same temperature range.[6] Below T_N, where long-range magnetic ordering takes place, Eqs. (A4) and (A7) gave, for a critical exponent $\beta=0.19$, an ordering temperature $T_N\cong 8.7$ K. The apparent discrepancy between the observed and calculated

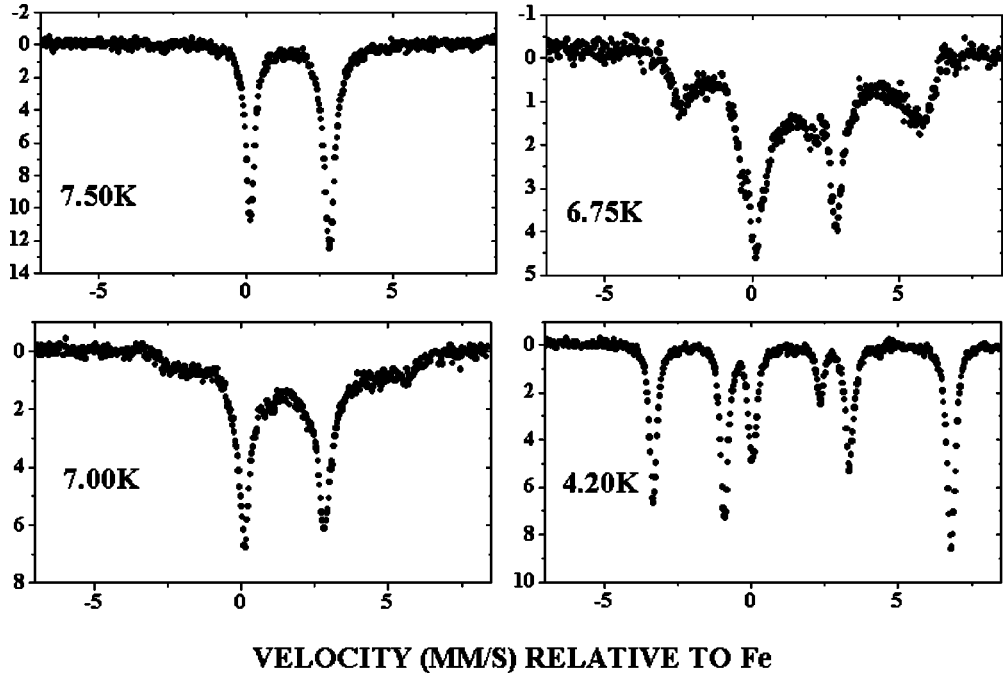

FIG. 9. Mössbauer spectra of the $Fe(NCS)_2(pyz\text{-}d_4)_2$ at various temperatures.

Néel temperature can be accounted for by the fact that the near-neighbor correlations remain anomalously strong even above T_N. This is consistent with other 2D Ising systems with a coupling J' between the layers, where an energy difference of $2J'N$, N being the average number of spins per domain within the layer, is observed.[18,22,26]

Finally we mention that the NPD and heat capacity values of $T_N=6.8$ K agree with our temperature-dependent Mössbauer data for $Fe(NCS)_2(pyz\text{-}d_4)_2$. In particular, the magnetic hyperfine splitting of this complex occurs for $T\simeq 7$ K, see Fig. 9, as opposed to between 8 and 9 K.[13]

IV. SUMMARY AND REMARKS

Using on one hand thermodynamic quantities that reflect the short-range order, and on the other hand the sublattice magnetization, we were able to conclude that although 3D ordering is achieved below T_N in $Fe(NCS)_2(pyz)_2$ the critical parameters are ideally close to the ones expected for 2D Ising systems,[28] and $Fe(NCS)_2(pyz)_2$ can be regarded as a 2D antiferromagnet even in the ordered phase. Indeed the magnetic order parameter follows the exact Onsager solution for a $S=1/2$ 2D Ising system with a critical exponent $\beta=0.19$. A well-defined dispersionless spin-wave gap is observed in the INS spectra. In addition, for $T<T_N$, the gap increases and scales with the sublattice magnetization. In the vicinity of the critical temperature the magnetic specific heat (C_m) can be well described by the Onsager prediction for a 2D Ising square $S=1/2$ system [Eq. (A8)] giving a J value of 0.25 meV.

Furthermore we should mention that, similarly to other layered compounds with Fe^{2+} as magnetic ion, such as K_2FeF_4 and Rb_2FeF_4, although exchange interaction is assumed to be dominant in $Fe(NCS)_2(pyz)_2$, easy-plane anisotropy plays an important role in defining the unique direction of the magnetic moments.[34]

An interesting modulation of the present system would consist of lightly doping the Fe site with a diamagnetic ion with the aim of decreasing the coherence length of the intralayer ordering and to study the doping threshold for which 3D ordering is quenched. Another alternative will be to use various size counteranions and thus modulate the interlayer coupling. In this context, we mention preliminary helium-3 Mössbauer spectroscopy studies[35] on $FeCl_2(pyz)_2$ which show that it magnetically orders near 0.5 K.

ACKNOWLEDGMENTS

We have benefited immensely from discussions of this work with J.W. Lynn (NIST). We gratefully acknowledge J. Rodríguez-Carvajal (LLB-Saclay) for advice regarding the magnetic structure determination and time-of-flight refinement with FULLPROF, B. Campbell (Argonne National Laboratory), for computing the grid search of the propagation vector with a modified form of the Wilkinson method, and E. A. Goremychkin for the preliminary INS measurements performed using LRMECS at the Intense Pulsed Neutron Source. The authors thank Simine Short, D. Többens, and K. Andersen for their assistance during the SEPD, *E*9, and OSIRIS measurements. HNB specially thanks R.E. Lechner (HMI) for the measurements on NEAT and T. Hicks (Monash University) for helpful discussions. This work was funded by the U.S. Department of Energy, BES-Materials Science, under Contract No. W-31-109-ENG-38. Oak Ridge National Laboratory is managed by UT-Battelle, LLC for the U. S. Department of Energy under Contract No DE-AC05-00OR22725.

APPENDIX

The 2D Ising system is the only low-dimensional system capable of exhibiting a phase transition for which an exact solution exists which was derived by Onsager.[14] This model gives an exact set of critical exponents for the $d=2$, $n=1$ universality class. The Hamiltonian is given as

$$H = -J\sum_{i,j} S_i \cdot S_j - h\sum_i S_i, \tag{A1}$$

where J is the coupling constant, which represents for the physical exchange energy, i,j represents the nearest-neighbor summations, and h is the temperature-dependent staggered magnetization responsible for the stabilization of the long-range magnetic order.

In the thermodynamic limit, and at zero field, the energy per spin is then given by

$$\varepsilon(T) = -2J\tanh\left(\frac{2J}{k_B T}\right) + \frac{K}{2\pi}\frac{dK}{d\theta}\int_0^{\pi} d\phi \frac{\sin^2\phi}{\Delta(1+\Delta)}, \tag{A2}$$

where

$$\Delta = \sqrt{1 - K^2\sin^2\phi} \tag{A3}$$

Hence for $T<T_N$, the magnetization becomes[29]

$$\frac{M(T)}{M_0} = \left\{1 - \left[\sinh\left(\frac{2J}{k_B T}\right)\right]^{-4}\right\}^{\beta} \quad \text{and} \quad \beta = \frac{1}{8}, \tag{A4}$$

indicating the presence of an order-disorder phase transition at zero field. M_0 represents the fully ordered moment at 0 K, $M(T)$ the moment at a given T, and k_B the Boltzmann constant.

The condition for determining the critical temperature at which the phase transition occurs is then given by the relation

$$\tanh^2(2J/k_B T_N) = 1, \quad \text{with} \quad k_B T_N \approx 2.269\,185 J. \tag{A5}$$

For $T>T_N$, and just below the onset of the 2D long-range order, the interaction between staggered magnetization of adjacent layers after renormalization of the exchange can be approximated by the 1D Ising model:[24]

$$M_{1D(T)} \sim \exp\frac{2J'}{T}. \tag{A6}$$

From spin-wave theory and antiferromagnetic resonance measurements it is well known from that for layer compounds[36–38] the gap $E_{k=0}$ scales with the sublattice magnetization as:

$$E_{k=0}(T) = E_{k=0}(0)\frac{M(T)}{M_0}. \tag{A7}$$

Furthermore the heat capacity per spin is given by

$$\frac{C_m(T)}{k_B} = \frac{8}{\pi}\left(\frac{J}{k_B T_N}\right)^2\left[-\ln\left(\frac{T_N - T}{T_N}\right) + \ln\left(\frac{k_B T_N}{2J}\right) - \left(1 + \frac{\pi}{4}\right)\right], \tag{A8}$$

which diverges logarithmically as $T \to T_N$.

*Electronic address: bordallo@hmi.de
†Electronic address: L.C.Chapon@rl.ac.uk

[1] See, for example, O. Kahn, *Molecular Magnetism* (John Wiley & Sons, New York, 1993).
[2] W. R. Entley and G. S. Girolami, Science **268**, 397 (1995).
[3] A. Santoro, A. D. Mighell, and C. W. Reimann, Acta Crystallogr., Sect. B: Struct. Crystallogr. Cryst. Chem. **26**, 979 (1970).
[4] P. W. Carreck, M. Goldstein, E. M. MacPartlin, and W. D. Unsworth, J. Chem. Soc., Chem. Commun. **1971**, 1634.
[5] J. Darriet, M. S. Haddad, E. N. Duester, and D. N. Hendrickson, Inorg. Chem. **18**, 2679 (1979).
[6] J. A. Real, G. D. Munno, M. C. Munoz, and M. Julve, Inorg. Chem. **30**, 2701 (1991).
[7] H. N. Bordallo, L. Chapon, J. L. Manson, C. D. Ling, J. S. Qualls, D. Hall, and D. Argyriou, Polyhedron **22**, 2045 (2003).
[8] J. S. Haynes, S. J. Rettig, J. R. Sams, R. C. Thompson, and J. Trotter, Can. J. Chem. **65**, 420 (1987).
[9] P. J. Hay, J. C. Thibeault, and R. Hoffman, J. Am. Chem. Soc. **97**, 4884 (1975).
[10] J. L. Manson, Q. Z. Huang, J. W. Lynn, H. J. Koo, M. H. Whangbo, R. Bateman, T. Otsuka, N. Wada, D. N. Argyriou, and J. S. Miller, J. Am. Chem. Soc. **13**, 162 (2001).
[11] H.-L. Sun, B.-Q. Ma, S. Gao, and G. Su, Chem. Commun. (Cambridge) **24**, 2586 (2001).
[12] B.-Q. Ma, H.-L. Sun, S. Gao, and G. Su, Chem. Mater. **13**, 1946 (2001). In this particular case the high T_N is due to a combination of both bridging azide and N,N'-pyrazine-dioxide ligands.
[13] J. C. Haynes, A. Kostikas, J. R. Sams, A. Simopoulos, and R. C. Thompson, Inorg. Chem. **26**, 2630 (1987).
[14] L. Onsager, Phys. Rev. **65**, 117 (1944).
[15] A. C. Larson and R. B. V. Dreele, General Structure Analysis (GSAS), Los Alamos National Laboratory Report L-UR-86–748 (1994).
[16] J. Rodriguez-Carvajal, Physica B **192**, 55 (1993).
[17] Because the sample angle was 135° the energy resolution increases at higher angles.
[18] S. Y. Wu, W.-H. Li, K. C. Lee, J. W. Lynn, T. H. Meen, and H. D. Yang, Phys. Rev. B **54**, 10019 (1996).
[19] J. Hernandez-Velasco (private communication). Recent HRTEM results indicate the existence of stacking faults along the *c* axis.
[20] B. E. Warren, Phys. Rev. **59**, 693 (1941).
[21] C. Wilkinson, G. Lautenschlager, R. Hock, and H. Weitzel, J. Appl. Crystallogr. **24**, 365 (1991).
[22] J. W. Lynn, T. W. Clinton, W.-H. Li, R. W. Erwin, J. Z. Liu, K. Vandervoort, and R. N. Shelton, Phys. Rev. Lett. **63**, 2606 (1989).
[23] G. Bottger, P. Fischer, A. Donni, Y. Aoki, H. Sato, and P. Berastegui, J. Magn. Magn. Mater. **177**, 517 (1998).

[24] D. Vaknin, J. L. Zarestky, J. E. Ostenson, B. C. Chakoumakos, A. Goni, P. Pagliuso, T. Rojo, and G. E. Barberis, Phys. Rev. B **60**, 1100 (1999).
[25] P. Nordblad, D. P. Belanger, A. R. King, V. Jaccarino, and H. Ikeda, Phys. Rev. B **28**, 278 (1983).
[26] R. J. Birgeneau, H. J. Guggenheim, and G. Shirane, Phys. Rev. B **8**, 304 (1973).
[27] J. Skalyo, G. Shirane, R. J. Birgeneau, and H. J. Guggenheim, Phys. Rev. Lett. **23**, 1394 (1969).
[28] S. T. Bramwell and P. C. W. Holdsworth, J. Appl. Phys. **73**, 6096 (1993).
[29] C. N. Yang, Phys. Rev. **85**, 808 (1952).
[30] S. Skanthakumar, J. W. Lynn, and F. Dogan, J. Appl. Phys. **81**, 4934 (1987).
[31] R. J. Birgeneau, F. D. Rosa, and H. J. Guggenheim, Solid State Commun. **8**, 13 (1970).
[32] M. P. H. Thurlings, E. Frikkee, and H. W. deWijn, Phys. Rev. B **25**, 4750 (1982).
[33] S. Fulton, S. E. Nagler, L. M. N. Needham, and B. M. Wanklyn, J. Phys.: Condens. Matter **6**, 6667 (1994).
[34] U. Balucani, M. G. Pini, and V. Tognetti, J. Phys. C **13**, 2925 (1980).
[35] W. M. Reiff, J. Li, M. A. Lawandy, C. C. Torardi, and T. Yuen, The VIIth International Conference on Molecular Magnetism, San Antonio, Texas (2000).
[36] H. W. deWijn, R. E. Walstedt, and H. J. Guggenheim, Phys. Rev. Lett. **24**, 832 (1970).
[37] H. W. deWijn, L. R. Walker, S. Geschwind, and H. J. Guggenheim, Phys. Rev. B **8**, 299 (1973).
[38] A. F. M. Arts and H. W. deWijn, Phys. Rev. B **15**, 4348 (1977).